

The consequences of inducing disorder in a high affinity protein-protein interaction

Grigorios A. Papadakos, Amit Sharma, Lorna Lancaster, Rebecca Bowen, Renata Kaminska, Andrew Leech, Daniel Walker, Christina Redfield, and Colin Kleanthous

J. Am. Chem. Soc., **Just Accepted Manuscript** • DOI: 10.1021/ja512607r • Publication Date (Web): 09 Apr 2015

Downloaded from <http://pubs.acs.org> on April 13, 2015

Just Accepted

“Just Accepted” manuscripts have been peer-reviewed and accepted for publication. They are posted online prior to technical editing, formatting for publication and author proofing. The American Chemical Society provides “Just Accepted” as a free service to the research community to expedite the dissemination of scientific material as soon as possible after acceptance. “Just Accepted” manuscripts appear in full in PDF format accompanied by an HTML abstract. “Just Accepted” manuscripts have been fully peer reviewed, but should not be considered the official version of record. They are accessible to all readers and citable by the Digital Object Identifier (DOI®). “Just Accepted” is an optional service offered to authors. Therefore, the “Just Accepted” Web site may not include all articles that will be published in the journal. After a manuscript is technically edited and formatted, it will be removed from the “Just Accepted” Web site and published as an ASAP article. Note that technical editing may introduce minor changes to the manuscript text and/or graphics which could affect content, and all legal disclaimers and ethical guidelines that apply to the journal pertain. ACS cannot be held responsible for errors or consequences arising from the use of information contained in these “Just Accepted” manuscripts.



The consequences of inducing intrinsic disorder in a high affinity protein-protein interaction

Papadakos, G.¹, Sharma, A.², Lancaster, L.E.³, Bowen, R.^{4‡}, Kaminska, R.¹, Leech, A.P.⁴, Walker, D.⁵, Redfield, C.¹ & Kleanthous, C.¹

¹Department of Biochemistry, University of Oxford, South Parks Road, Oxford, OX1 3QU, United Kingdom

²Astbury Centre for Structural Molecular Biology, University of Leeds, Leeds LS2 9JT United Kingdom

³School of Life Sciences, University of Lincoln, Brayford Pool, Lincoln, LN6 7TS, United Kingdom

⁴Department of Biology, University of York, Heslington Road, YO10 5DD, United Kingdom

⁵Institute of Infection, Immunity and Inflammation, College of Medical, Veterinary and Life Sciences, University of Glasgow, Glasgow, G12 8AT, United Kingdom

‡Current address: Oxford Nanopore Technologies, Oxford Science Park, Edmund Cartwright house, Oxford, OX4 4GA, United Kingdom

Supporting Information Placeholder

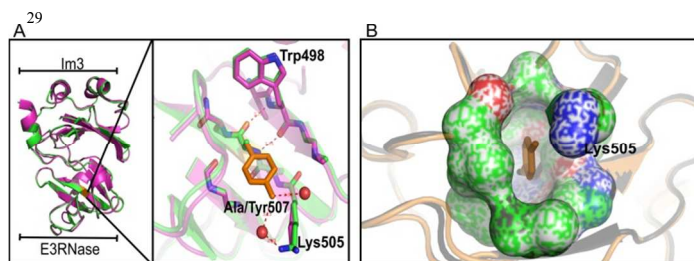
ABSTRACT: The kinetic and thermodynamic consequences of intrinsic disorder in protein-protein recognition are controversial. We addressed this problem by inducing one partner of the high-affinity colicin E3 rRNase domain-Im3 complex ($K_d \sim 10^{-12}$ M) to become an intrinsically disordered protein (IDP). Through a variety of biophysical measurements we show that a single alanine mutation at Tyr507 within the hydrophobic core of the isolated colicin E3 rRNase domain causes the enzyme to become an IDP (E3 rRNase^{IDP}). E3 rRNase^{IDP} binds stoichiometrically to Im3 and forms a structure that is essentially identical to the wild-type complex. However, E3 rRNase^{IDP} binds Im3 four-orders-of-magnitude weaker than the folded rRNase, with thermodynamic parameters reflecting the disorder-to-order transition on forming the complex. Critically, pre-steady state kinetic analysis of the E3 rRNase^{IDP}-Im3 complex demonstrates that the decrease in affinity is mostly accounted for by a drop in the electrostatically-steered association rate. Our study shows that notwithstanding the advantages intrinsic disorder brings to biological systems this can come at severe kinetic and thermodynamic cost.

IDPs are found in all domains of life where they play central roles in a multitude of biological processes, including transcription, translation, cell division and cell death.¹⁻⁴ IDPs are also implicated in a number of human diseases such as cancer, Alzheimer's, Parkinson's and type II diabetes.⁵⁻⁸ The functional repertoire of IDPs is similarly diverse, ranging from flexible linkers between domains, sites of post-translational modification, chaperones for proteins and nucleic acids, hubs in protein-protein interaction (PPI) networks and membrane translocation modules.⁹⁻¹¹ IDP assembly is critical to the recently described phenomenon of liq-

uid-to-liquid phase transitions within cells and has been exploited in the generation of novel biomaterials.¹² Given the importance of IDPs to biology, medicine and biotechnology there is great interest in understanding their mechanisms of association with other macromolecules. Since IDPs have been retained in biological systems over evolutionary time this implies they endow these systems with particular advantages over their globular counterparts.¹⁰ One of the often cited advantages of IDPs in PPIs is their faster association rate, due to a larger capture radius, the so-called "fly-casting" mechanism, and fewer encounters on the path to the final complex.¹³ However, beyond surveys of association rate data for IDP and globular protein complexes and theoretical predictions, there has been no direct experimental test of this effect presumably because of the difficulty in comparing the *same* PPI for a globular and IDP complex. The present work set out to address this problem using the colicin ribonuclease E3 and its specific immunity protein, Im3.

Colicin E3 (ColE3) is a ribosomal RNase (rRNase) toxin released by *Escherichia coli* cells to kill their neighbours during times of environmental stress. The 12-kDa E3 rRNase domain is delivered to the cytoplasm of susceptible bacteria where it cleaves the phosphodiester bond between A1493 and G1494 within the decoding centre of the ribosomal A-site, leading to the inhibition of protein synthesis and cell death.^{14,15} ColE3-producing bacteria are protected against the action of the rRNase and hence suicide by the 9.8 kDa immunity protein Im3. Im3 binds with very high affinity ($K_d = 10^{-12}$ M, pH 7.0, 200 mM NaCl and 25°C) to the isolated E3 rRNase domain, only dissociating from the enzyme during colicin import.^{16,17} Interestingly, the Im3-E3 rRNase complex has some features associated with IDP complexes; Im3 makes contact with long contiguous segments of the E3 rRNase polypeptide including

1 the N-terminal α -helix, a long linker sequence that lacks regular
 2 secondary structure and two short strands of β -sheet.¹⁸
 3 Previously, we have shown, using far-UV circular dichroism (CD)
 4 and tryptophan emission fluorescence spectroscopy, that an ala-
 5 nine mutant of Tyr507 within the hydrophobic core of the rRNase
 6 destabilizes the enzyme.¹⁹ Here, closer analysis of this mutant by
 7 differential scanning calorimetry, near-UV CD, analytical ultra-
 8 centrifugation and high-field NMR spectroscopy, indicated that
 9 Y507A E3 rRNase was unfolded at room temperature and hence
 10 had become a *de facto* IDP (E3 rRNase^{IDP}; **Figure S1**). In fact a
 11 significant proportion of the ColE3 rRNase domain is predicted to
 12 be disordered (35 and 50% using PONDR-VLXT and PRDos,
 13 respectively), a consequence of its high glycine, lysine and proline
 14 content (17, 18 and 9%, respectively). It is perhaps unsurprising
 15 therefore that although the E3 rRNase is clearly a folded domain
 16 ($\Delta G_{\text{stabilization}}$, -9.2 kcal/mol by DSC; **Figure S1**) a single Tyr-to-
 17 Ala mutation within its hydrophobic core is sufficient to render it
 18 an IDP. We determined the hydrodynamic radius of E3
 19 rRNase^{IDP} by NMR spectroscopy (25.6 Å) and found it midway
 20 between that of the native domain (20.1 Å) and E3 rRNase un-
 21 folded in 8 M urea (30.2 Å) suggesting that like other IDPs,²⁰ E3
 22 rRNase^{IDP} is more compact than the urea-denatured state. Its
 23 compact shape might arise from its high glycine and proline con-
 24 tent as previously observed for IDPs.^{21,22} No changes in the hy-
 25 drodynamic radius of the E3 rRNase^{IDP} were observed across a
 26 range of 0-500 mM NaCl so, unlike other IDPs,^{21,23} its relative
 27 compactness is probably not due to favorable intramolecular
 28 charge-charge interactions.



37 **Figure 1.** The E3 rRNase^{IDP} (Y507A) folds into a native-like structure upon binding to its cognate
 38 partner Im3. (A) Superposed cartoon models of the wild-type (magenta) and Im3- E3 rRNase^{IDP}
 39 complex (green) highlighting the structural similarity between the two complexes (inset), and the
 40 ball and stick model showing the disposition of residues in a 5Å sphere around Tyr/Ala507. Also
 41 shown are the H-bond interactions of Ala/Tyr507 and associated water molecules that are lost in
 42 the alanine mutant. (B) Surface representation of residues in a 5Å sphere highlighting the hole
 43 created when Tyr507 is substituted for alanine.

44
 45 We next examined the ability of E3 rRNase^{IDP} to bind Im3. Tryptop-
 46 hophan fluorescence emission spectroscopy, sedimentation veloci-
 47 ty analytical ultracentrifugation and ¹H-¹⁵N HSQC NMR spec-
 48 troscopy showed E3 rRNase^{IDP} bound Im3 stoichiometrically
 49 (**Figure S2A-C**). We also crystallized the E3 rRNase^{IDP}-Im3
 50 complex and solved its structure at 2.97 Å resolution by molecular
 51 replacement (see **Table S1** for refinement statistics). The root
 52 mean square deviation for backbone atoms of a structural super-
 53 position of the wild-type and E3 rRNase^{IDP} was 0.36 Å² (for 96
 54 residues) indicating that upon binding Im3 the E3rRNase^{IDP} folds
 55 to a conformation identical to that of the wild type protein (**Fig.**
 56 **1A**). Indeed, every hydrogen bond, hydrophobic and electrostatic
 57 interaction associated with the binding interface of the complex is
 58 preserved. The major differences between the structures are lo-
 59 calized to the mutation site within the hydrophobic core of the E3
 60 rRNase although even here the backbone conformation of wild-
 61 type E3 rRNase and the E3 rRNase^{IDP} are near identical, empha-
 62 sized by the conserved hydrogen bonding interactions involving
 63 the main-chain atoms of residue 507 with Trp498 (**Fig. 1A**). The
 64 only substantial differences between the wild-type and mutant

65 complex is the creation of a 213 Å³ cavity (**Fig. 1B**), accounting
 66 for 3.4% of the hydrophobic core of the E3 rRNase, and the loss
 67 of two ordered water molecules that are coordinated to the phe-
 68 nolic hydroxyl of Tyr507 (**Fig. 1A**). We conclude that it is the
 69 loss of these interactions which renders the unliganded E3
 70 rRNase^{IDP} predominantly unfolded at room temperature. We note
 71 that complexes involving IDPs are sometimes ‘frustrated’²⁴ and so
 72 a cavity within the core of the E3 rRNase^{IDP} merely represents
 73 another form of frustration.

74 Having established that the complex formed between E3
 75 rRNase^{IDP} and Im3 is essentially identical to that formed by the
 76 wild type enzyme, we embarked on a thermodynamic and kinetic
 77 dissection of the complex. Isothermal titration calorimetry (ITC)
 78 demonstrated that the thermodynamic consequence of inducing
 79 the E3 rRNase to become an IDP (at pH 7.0 and 25°C) was a
 80 four-orders-of-magnitude increase in the equilibrium dissociation
 81 constant with respect to the wild type complex; K_d , 28 nM com-
 82 pared to 1.2 pM at 25°C pH 7.0, 200 mM NaCl (**Figure S2D** and
 83 **Table 1**). Concomitant with this decrease in affinity is a complete
 84 change in the thermodynamic profile of the complex. Whereas a
 85 favourable enthalpy and entropy drive complex formation of the
 86 folded proteins, the E3 rRNase^{IDP}-Im3 complex has a strongly
 87 disfavoured entropy that is compensated by a large increase in the
 88 enthalpic component. These thermodynamic features of the E3
 89 rRNase^{IDP}-Im3 complex are typical of binding-induced folding
 90 described for many complexes involving IDPs. The large entrop-
 91 ic penalty is due to the loss of intra-molecular conformational
 92 degrees of freedom due to folding which in this case is only partly
 93 compensated by the favorable desolvation of the exposed hydro-
 94 phobic core of the E3 rRNase (-25 kcal/mol for E3 rRNase^{IDP}
 95 compared to +3.2 kcal/mol in the case of the wild type E3). The
 96 large favourable enthalpy reflects simultaneously the non-
 97 covalent interactions that stabilize the folded state of the enzyme
 98 as well as the extensive network of interactions between the two
 99 proteins at the protein-protein interface (**Table 1**). A further strik-
 100 ing difference between the E3 rRNase^{IDP}-Im3 and wild type com-
 101 plexes is the much weaker ionic strength dependence for the com-
 102 plex involving the IDP. Wild type E3 rRNase affinity for Im3 is
 103 reduced by almost three-orders-of-magnitude over a NaCl concen-
 104 tration range of 20-500 mM,¹⁷ whereas E3 rRNase^{IDP} affinity is
 105 only affected 20-fold.

Table 1 E3 rRNase-Im3 binding energetics determined by ITC^a

NaCl (mM)	20	200	500	
E3 rRNase	IDP	WT ^b	IDP	
ΔH	-41.0 ± 1.6	-13.0	-35.0 ± 6.0	-31.0 ± 4.5
TAS	-29.6 ± 1.6	3.2	-24.8 ± 6.2	-21.0 ± 4.6
ΔG	-11.4	-16.2	-10.2	-10.0
K_d (M)	4.0 × 10 ⁻⁹	1.2 × 10 ⁻¹²	2.8 × 10 ⁻⁸	× 10 ⁻⁸

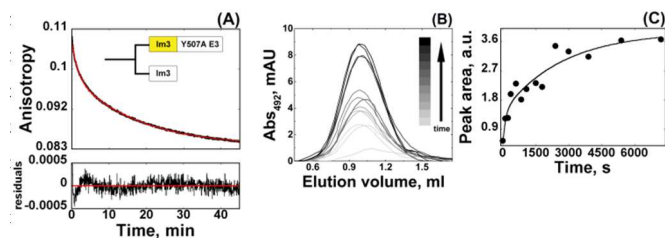
(a) Energies expressed in kcal/mol and all binding experiments performed in 50 mM MOPS-NaOH, pH 7.0 at 25°C and the indicated salt concentrations. (b) WT, wild type values taken from reference 17.

106

107 We next investigated the impact of inducing E3 rRNase to be-
 108 come an IDP on the kinetics of complex formation with Im3. The
 109 wild type complex is characterized by a very rapid, salt-dependent
 110 bimolecular association ($k_{\text{on}} \sim 10^8 \text{ M}^{-1}\text{s}^{-1}$) in 50 mM MOPS-
 111 NaOH, 200 mM NaCl at 25°C and pH 7.0 and a slow, salt-
 112 independent dissociation. In the present work, we measured dis-
 113 sociation of the E3 rRNase^{IDP}-Im3 complex using Alexa⁴⁸⁸ modi-
 114 fied-Im3 in which the native cysteine (Cys47) was substituted for
 115 serine and a Glu-to-Cys mutation was created at position 53 for
 116 Alexa⁴⁸⁸ labelling. Position 53 was chosen as this is distant from
 117 the E3 rRNase binding site. ITC experiments indicated that Im3-
 118 Alexa⁴⁸⁸ bound E3 rRNase^{IDP} with low nanomolar affinity as for
 119 wild type Im3 (data not shown). Competition experiments were

2

1 set up where the E3 rRNase^{IDP}-Im3-Alexa⁴⁸⁸ complex was incu-
 2 bated with an excess of unlabeled Im3 in 50 mM MOPS-NaOH,
 3 pH 7.0 at various NaCl concentrations. The release of Im3-
 4 Alexa⁴⁸⁸ was followed either by fluorescence anisotropy in a
 5 stopped-flow device (T-mode) upon excitation at 470 nm or by
 6 absorbance of released Im3-Alexa⁴⁸⁸ at 492 nm following nickel-
 7 affinity chromatography. Biphasic dissociation profiles were
 8 obtained by both approaches, in contrast to the single phase ob-
 9 served for the wild-type complex (**Figure 2A-C**).¹⁷ The biphasic
 10 traces were fitted to a double exponential equation from which the
 11 amplitudes were estimated to differ by the same magnitude in the
 12 two experimental setups (~2.5-fold) suggesting both experiments
 13 were monitoring the same dissociation-induced processes. The
 14 average values of the two dissociation rate constants for the E3
 15 rRNase^{IDP}-Im3-Alexa⁴⁸⁸ complex (k_{off}^1 and k_{off}^2), corresponding
 16 to the higher and lower amplitudes, were $3.4 \times 10^{-4} \text{ s}^{-1}$ and $0.5 \times$
 17 10^{-4} s^{-1} , respectively, in 50 mM MOPS-NaOH, 200 mM NaCl at
 18 25°C and pH 7.0. Both rates were independent of the competing
 19 ligand concentration and both exhibited a mild dependence on
 20 NaCl concentration (**Table 2**). Importantly, both rate constants
 21 approximate that of the wild type complex under equivalent con-
 22 ditions ($k_{\text{off}} = 1.5 \times 10^{-4} \text{ s}^{-1}$).¹⁷ We conclude that while inducing
 23 the E3 rRNase to become an IDP increases the complexity of its
 24 dissociation mechanism from its complex with Im3, likely involv-
 25 ing different conformational states, it has a minimal impact on the
 26 overall rate of dissociation.

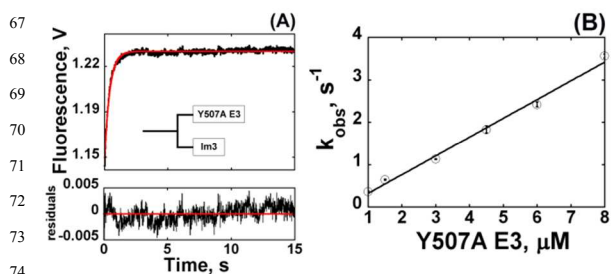


33 Figure 2. Dissociation of the E3 rRNase^{IDP}-Im3 complex measured through competition with
 34 Im3. (A) The time dependence of the anisotropy change for the dissociation of a 0.5 μM E3
 35 rRNase^{IDP}-Alexa-Im3 complex chased by 5 μM unlabeled Im3. Upon excitation at 470 nm the
 36 anisotropy of Alexa-Im3 was monitored in T-mode with a 515 nm cutoff filter set before each
 37 detector. The data were fit to a double exponential equation (Eq. 2, red). (B) The time depend-
 38 ence of the Ni-NTA elution peak corresponding to the released Alexa-Im3 (492 nm) upon dissoci-
 39 tion of a 2 μM E3 rRNase^{IDP}-Alexa-Im3 complex chased by 20 μM unlabeled Im3. (C) Fit of the
 40 integrated areas in (B) to a double exponential equation (Eq. 2). All experiments performed in 50
 41 mM MOPS-NaOH, 200 mM NaCl, pH 7.0 at 25°C.

42

43 The association kinetics of E3 rRNase^{IDP} with Im3 was deter-
 44 mined using stopped-flow tryptophan fluorescence, capitalizing
 45 on the significant enhancement in fluorescence emission that oc-
 46 curs on complex formation (**Figure S2A**). A single bimolecular
 47 step was observed under pseudo first-order conditions, without
 48 any detectable intermediates, from which an apparent association
 49 rate constant of $4.4 \times 10^5 \text{ M}^{-1} \text{ s}^{-1}$ was obtained (**Figure 3A, B**).
 50 With regards to the kinetic mechanism of the E3 rRNase^{IDP}-Im3
 51 complex, kinetic modelling using the apparent rate constants for
 52 association and dissociation (data not shown) has thus far been
 53 unsuccessful in furnishing an equilibrium dissociation constant
 54 from which we infer additional, spectroscopically silent steps are
 55 involved in complex formation. Nevertheless, our results demon-
 56 strate that for one partner to become an IDP has a profound im-
 57 pact on the kinetics of complex formation. First and foremost the
 58 association rate constant for the E3 rRNase^{IDP}-Im3 complex de-
 59 creased by three-orders-of-magnitude relative to the wild-type
 60 complex under the same conditions (**Table 2**).¹⁷ This is a particu-
 61 larly striking result given theoretical predictions suggesting IDPs
 62 have a kinetic advantage in forming protein-protein complexes.
 63 However, in this instance a further contributory factor impacts on
 64 association, which is the role of electrostatics. Association of

65 wild type E3 rRNase with Im3 is strongly electrostatically driven,
 66 demonstrated by the three-order-of-magnitude decrease in the



75 Figure 3. E3 rRNase^{IDP}-Im3 association monitored by stopped-flow fluorescence spectroscopy in
 76 50 mM MOPS-NaOH, 200 mM NaCl, pH 7.0 at 25°C. (A) Time dependence of the tryptophan
 77 fluorescence emission upon excitation at 295 nm under pseudo-first order conditions: 0.2 μM Im3
 78 mixed with 8 μM E3 rRNase^{IDP}. (B) The dependence of the observed rate constants under pseu-
 79 do-first order conditions (tryptophan emission experiments) on the concentration of E3 rRNase^{IDP}
 80 and its linear regression according to Eq. 3 (black line) which yields a bimolecular association
 81 constant at $4.4 \times 10^5 \text{ M}^{-1} \text{ s}^{-1}$.

82 association rate constant when the NaCl concentration is in-
 83 creased from 0-500 mM.¹⁷ Such strong salt dependence is typical
 84 of long range electrostatic steering, observed in many complexes
 85 involving oppositely charged proteins such as barnase-barstar and
 86 the colicin E9 DNase-Im9 complexes. The E3 rRNase is a basic
 87 protein (pI 9.9), with an overall charge of +11 [13 Asp + Glu/24
 88 Arg + Lys], while Im3 is acidic, with an overall charge of -14 [20
 89 Asp + Glu/6 Arg + Lys] at neutral pH. Even though the charge
 90 state for the E3 rRNase^{IDP} mutant is identical to the wild type
 91 protein there is now only a modest ionic strength dependence in
 92 its association rate with Im3, which decreases by only an order of
 93 magnitude between 20-200 mM NaCl (**Table 2**).

Table 2 E3 rRNase^{IDP}-Im3 association and dissociation kinetic rates

NaCl (mM)	20	200	500
$k_{\text{on}} (\times 10^5 \text{ M}^{-1} \text{ s}^{-1})$	40 ± 3.2	4.4 ± 0.2	1.2 ± 0.02
$k_{\text{off}}^1 (\times 10^{-4} \text{ s}^{-1})$	$2.3 (\pm 1.7)^a$	$3.1 (\pm 0.01)^a$ $3.7 (\pm 2.4)^b$	$3.8 (\pm 0.02)^a$
$k_{\text{off}}^2 (\times 10^{-3} \text{ s}^{-1})$	$4.6 (\pm 0.08)^a$	$6.3 (\pm 0.04)^a$ $4.3 (\pm 2.0)^b$	$7.3 (\pm 0.04)^a$

Values determined by fluorescence anisotropy (a) and the chromatographic release of Alexa-Im3 (b). Experiments performed in 50 mM MOPS-NaOH, pH 7.0 at 25°C and the indicated salt concentrations. Values for k_{on} and k_{off} for the wild-type complex in 200 mM NaCl under identical buffer conditions are $1.1 \times 10^8 \text{ M}^{-1} \text{ s}^{-1}$ and $1.5 \times 10^{-4} \text{ s}^{-1}$.¹⁷

94

95 This implies that the electrostatic steering responsible for enhanc-
 96 ing its association with Im3 is reduced on becoming an IDP. It
 97 has previously been demonstrated that charge complementarity
 98 plays a minor role in accelerating the association rates of short
 99 IDP fragments binding folded, globular protein partners.^{25,26} In
 100 the present case, we see that the same principle applies for a large,
 101 highly charged IDP (E3 rRNase^{IDP}) that in its folded state experi-
 102 ences marked electrostatic steering when binding its acidic partner
 103 Im3.¹⁷ Yet as an ensemble of rapidly interconverting conformers
 104 (**Fig. S1E**), the ‘polyelectrostatic effect’^{27,28} predicts that
 105 rRNase^{IDP} should experience electrostatic steering. Consequently
 106 the formation of a potential encounter Im3-E3 rRNase^{IDP} complex
 107 where the rRNase folds upon binding cannot be electrostatically
 108 driven. For steering to occur, the E3 rRNase needs to be natively
 109 folded before associating with Im3. The decrease in k_{on} could
 110 reflect the low concentration in the IDP ensemble of a ‘binding-
 111 competent, native-like’ conformation of E3 rRNase^{IDP}. In 200
 112 mM NaCl this species would have to represent 0.4% of the en-
 113 semble if it had the same k_{on} as the native E3 rRNase. Such a
 114 ‘native-like’ species present in the IDP ensemble would be ex-
 115 pected to show the same very strong electrostatic steering ob-
 116 served for the native protein; this is not observed. Thus, the
 117 change in NaCl concentration would have to have opposite ef-

3

1 facts; increasing salt diminishes electrostatic steering but at the
2 same time increases the population of the binding-competent na-
3 tive-like state (from 0.03% at 20 mM NaCl to 0.4% at 200 mM
4 NaCl to 0.75% at 500 mM NaCl). These very small populations
5 of a binding-competent state are almost impossible to detect by
6 any biophysical method. Relaxation dispersion methods are often
7 used to detect low population ‘excited’ states in a conformational
8 ensemble. No evidence for such a species in E3 rRNase^{IDP} could
9 be detected using ¹⁵N relaxation dispersion. In addition, no
10 change in the hydrodynamic radius of the IDP ensemble was ob-
11 served between 0 and 500 mM NaCl.

12 To date, the kinetic and thermodynamic merits of IDPs in protein-
13 protein complexes have been established via their comparison
14 with folded proteins that bind to the same partner. Our work pro-
15 vides unique insight into the consequences of disorder on a high
16 affinity complex through direct comparison of the ordered and
17 disordered states binding the same partner. We highlight the pos-
18 sibility that plasticity and larger hydrodynamic radius may actual-
19 ly decrease the association rate by diminishing the influence of
20 charge on the formation of the encounter complex between a
21 highly charged IDP and its folded counterpart. This is in contrast
22 to the ‘fly-casting’ mechanism,¹³ which is often used to explain
23 diffusion limited association rates for IDP complexes.²⁹⁻³⁴

24 ASSOCIATED CONTENT

25 Supporting Information

26 Figures S1 and S2 along with detailed experimental procedures
27 are included in the Supporting Information. This material is
28 available free of charge via the Internet at <http://pubs.acs.org>.

29 AUTHOR INFORMATION

30 Corresponding Author

31 colin.kleanthous@bioch.ox.ac.uk

32 Notes

33 The authors declare no competing financial interests.

34 ACKNOWLEDGMENT

35 This work was supported by a grant from the Biotechnology and
36 Biological Sciences Research Council of the UK
37 (BB/G020671/1). We would like to acknowledge ESRF ID144 for
38 providing us with beam time.

39 REFERENCES

- 40 (1) Dyson, H. J.; Wright, P. E. *Nat.Rev.Mol.Cell Biol.* **2005**, *6*,
41 197.
42 (2) Uversky, V. N. *Int J Biochem Cell Biol* **2011**, *43*, 1090.
43 (3) Uversky, V. N. *Chemical reviews* **2014**, *114*, 6557.
44 (4) Ward, J. J.; Sodhi, J. S.; McGuffin, L. J.; Buxton, B. F.;
45 Jones, D. T. *J Mol Biol* **2004**, *337*, 635.
46 (5) Knowles, T. P.; Vendruscolo, M.; Dobson, C. M. *Nature*
47 *reviews. Molecular cell biology* **2014**, *15*, 384.
48 (6) Larsen, R. A.; Chen, G. J.; Postle, K. *J Bacteriol* **2003**, *185*,
49 4699.
50 (7) Westermarck, P.; Wernstedt, C.; Wilander, E.; Hayden, D. W.;
51 O'Brien, T. D.; Johnson, K. H. *Proc Natl Acad Sci U S A* **1987**,
52 *84*, 3881.
53 (8) Xue, B.; Uversky, V. N. *J Mol Biol* **2014**, *426*, 1322.
54 (9) van der Lee, R.; Buljan, M.; Lang, B.; Weatheritt, R. J.;
55 Daughdrill, G. W.; Dunker, A. K.; Fuxreiter, M.; Gough, J.;

- 56 Gsponer, J.; Jones, D. T.; Kim, P. M.; Kriwacki, R. W.; Oldfield,
57 C. J.; Pappu, R. V.; Tompa, P.; Uversky, V. N.; Wright, P. E.;
58 Babu, M. M. *Chemical reviews* **2014**, *114*, 6589.
59 (10) Liu, Z.; Huang, Y. *Protein Sci* **2014**, *23*, 539.
60 (11) Housden, N. G.; Hopper, J. T.; Lukoyanova, N.; Rodriguez-
61 Larrea, D.; Wojdyla, J. A.; Klein, A.; Kaminska, R.; Bayley, H.;
62 Saibil, H. R.; Robinson, C. V.; Kleanthous, C. *Science* **2013**, *340*,
63 1570.
64 (12) Toretsky, J. A.; Wright, P. E. *The Journal of cell biology*
65 **2014**, *206*, 579.
66 (13) Shoemaker, B. A.; Portman, J. J.; Wolynes, P. G. *Proc Natl*
67 *Acad Sci U S A* **2000**, *97*, 8868.
68 (14) Bowman, C. M.; Dahlberg, J. E.; Ikemura, T.; Konisky, J.;
69 Nomura, M. *Proc.Natl.Acad.Sci.U.S.A* **1971**, *68*, 964.
70 (15) Ng, C. L.; Lang, K.; Meenan, N. A.; Sharma, A.; Kelley, A.
71 C.; Kleanthous, C.; Ramakrishnan, V. *Nat Struct Mol Biol* **2010**,
72 *17*, 1241.
73 (16) VanKemmelbeke, M.; Zhang, Y.; Moore, G. R.; Kleanthous,
74 C.; Penfold, C. N.; James, R. *The Journal of biological chemistry*
75 **2009**, *284*, 18932.
76 (17) Walker, D.; Moore, G. R.; James, R.; Kleanthous, C.
77 *Biochemistry* **2003**, *42*, 4161.
78 (18) Carr, S.; Walker, D.; James, R.; Kleanthous, C.; Hemmings,
79 A. M. *Structure* **2000**, *8*, 949.
80 (19) Walker, D.; Lancaster, L.; James, R.; Kleanthous, C. *Protein*
81 *Sci* **2004**, *13*, 1603.
82 (20) Uversky, V. N. *Biochimica et biophysica acta* **2013**, *1834*,
83 932.
84 (21) Marsh, J. A.; Forman-Kay, J. D. *Biophys J* **2010**, *98*, 2383.
85 (22) Tran, H. T.; Mao, A.; Pappu, R. V. *Journal of the American*
86 *Chemical Society* **2008**, *130*, 7380.
87 (23) Muller-Spath, S.; Soranno, A.; Hirschfeld, V.; Hofmann, H.;
88 Ruegger, S.; Reymond, L.; Nettels, D.; Schuler, B. *Proc Natl*
89 *Acad Sci U S A* **2010**, *107*, 14609.
90 (24) Jemth, P.; Mu, X.; Engstrom, A.; Dogan, J. *J Biol Chem*
91 **2014**, *289*, 5528.
92 (25) Shammas, S. L.; Travis, A. J.; Clarke, J. *The journal of*
93 *physical chemistry. B* **2013**, *117*, 13346.
94 (26) Sugase, K.; Dyson, H. J.; Wright, P. E. *Nature* **2007**, *447*,
95 1021.
96 (27) Borg, M.; Mittag, T.; Pawson, T.; Tyers, M.; Forman-Kay, J.
97 D.; Chan, H. S. *Proc Natl Acad Sci U S A* **2007**, *104*, 9650.
98 (28) Mittag, T.; Orlicky, S.; Choy, W. Y.; Tang, X.; Lin, H.;
99 Sicheri, F.; Kay, L. E.; Tyers, M.; Forman-Kay, J. D. *Proc Natl*
100 *Acad Sci U S A* **2008**, *105*, 17772.
101 (29) Chemes, L. B.; Sanchez, I. E.; de Prat-Gay, G. *J Mol Biol*
102 **2011**, *412*, 267.
103 (30) Dogan, J.; Schmidt, T.; Mu, X.; Engstrom, A.; Jemth, P. *J*
104 *Biol Chem* **2012**, *287*, 34316.
105 (31) Ganguly, D.; Otieno, S.; Waddell, B.; Iconaru, L.; Kriwacki,
106 R. W.; Chen, J. *J Mol Biol* **2012**, *422*, 674.
107 (32) Rogers, J. M.; Steward, A.; Clarke, J. *Journal of the*
108 *American Chemical Society* **2013**, *135*, 1415.
109 (33) Shammas, S. L.; Travis, A. J.; Clarke, J. *Proc Natl Acad Sci*
110 *U S A* **2014**, *111*, 12055.
111 (34) Arai, M.; Ferreone, J. C.; Wright, P. E. *Journal of the*
112 *American Chemical Society* **2012**, *134*, 3792.

Table of Contents artwork

